Journal of Engineering Research and Education
Volume 15, 2023 [37-48]

Investigating the Effectiveness of Maximum Power Point Tracking (MPPT) with Perturb and Observe (P&O) Algorithm in Solar Power Battery Charging System

Mohd Nadzim Mat Yusoof[1], Muhammad Iqbal Zakaria[1*], Ezreen Farina Shair[2], Nurul Syahirah Khalid[3] and Abdul Rahman A.A Emhemed[4]

[1]School of Electrical Engineering, College of Engineering, Universiti Teknologi MARA, Shah Alam, Malaysia
[2]Rehabilitation Engineering and Assistive Technology Research Group, Center for Robotics and Industrial Automation, Faculty of Electrical Engineering, Universiti Teknikal Malaysia Melaka, Durian Tunggal, Malaysia
[3]Faculty of Electrical Engineering & Technology, Universiti Malaysia Perlis, Kampus Pauh Putra, Arau, Perlis, Malaysia
[4]College of Technical Engineering, Bright Star University, El-Brega, Libya

ABSTRACT

Solar energy has emerged as one of the most promising and crucial renewable energy sources in our efforts to reduce reliance on fossil fuels and mitigate their adverse impact on the environment. One of the primary applications of solar energy is in the solar power battery charging system. This system harnesses solar energy emitted by the sun through solar panels to charge batteries used as energy storage. At the heart of the solar power battery charging system lies the technology of Maximum Power Point Tracking (MPPT). MPPT is a method used to achieve maximum efficiency from solar panels by adjusting their voltage and current to ensure they constantly operate at their maximum power point, irrespective of varying light conditions. In this article, the solar power battery charging system with the use of the MPPT method employing the Perturb and Observe (P&O) algorithm will be explored. The proposed of modeling the solar battery charging system with the implementation of a DC-DC buck converter and lead-acid battery incorporated with P&O algorithm will be elaborated through MATLAB/Simulink simulation software. Additionally, the performance analysis of the system will be investigated by considering the state of charge (SOC), power (W), current (A), and voltage (V) variables. The simulation results indicate the effectiveness of the proposed P&O algorithm in maintaining the panel's operating maximum power in multi-stage charging system.

Keywords: Battery charging, Four-stage charging system, Maximum Power Point Tracking, Photovoltaic system, P&O algorithm

1. INTRODUCTION

Solar photovoltaics (PV) has emerged as the world's fastest-growing energy technology, witnessing a significant rise in the global market over recent years. This exponential growth can be attributed to the continuous reduction in photovoltaic module costs over the past decade [1], [2], aligned with Sustainable Development Goals (SDG) [3]. Solar power is an effective tool against greenhouse gases, effectively curbing climate change, while its effortless installation, scalability, minimal maintenance, and versatile applications contribute to its widespread popularity. While solar panels rely on sunlight for efficient energy capture, energy storage solutions, such as batteries, offer an effective means to address the intermittency of solar power. By storing the surplus energy generated by the PV panels, batteries ensure a continuous and reliable energy supply even during periods of reduced sunlight [4], [5].

In solar PV systems, maintaining peak power output amidst changing environmental conditions

*Corresponding Author: iqbal.z@uitm.edu.my

is a challenge. Efficient Maximum Power Point Tracking (MPPT) technology is essential for optimal performance, enhancing energy capture from diverse solar irradiance conditions. This technology ensures solar panels operate at their peak power point by adjusting voltage and current [6]. The MPPT system precisely tracks maximum power output, efficiently delivering it to the battery charge controller. A multi-stage charging method [7] is employed, preventing battery damage from excessive charging [8].

Various methods of MPPT effectively optimize solar panel performance in diverse environmental conditions. Among them, the Incremental Conductance (IC) method [9] excels due to its precise tracking of the maximum power point, even in varying weather. IC utilizes instantaneous conductance changes to swiftly locate the power point. However, its hardware complexity could be a limitation, demanding sophisticated components [12], [13]. Another method, Fuzzy Logic Control (FLC) [10], mimics human decision-making, excelling in dynamic solar systems. FLC handles non-linearity, adapting to environmental changes. It operates without needing a strict mathematical model, simplifying implementation [14].

Artificial Neural Network (ANN) is a robust MPPT method [11] inspired by the human brain's neural networks. It adapts to varying environmental conditions, especially suitable for dynamic solar systems. Notably, ANN learns from historical data to optimize solar panel performance and energy capture. With applications in complex problem-solving, it addresses difficulties like particle interactions. The architecture of an ANN typically consists of three layers: input, hidden, and output layers [15]. In MPPT, ANN excels in optimizing solar panel performance using input data like voltage, current, irradiance, and temperature [16], [17]. Integrating ANN in MPPT is a major advancement, enhancing solar system efficiency and performance.

The Perturbation and Observation (P&O) method is a highly efficient MPPT technique. It continuously tracks the PV panel's Maximum Power Point (MPP), adapting to varying conditions irrespective of atmospheric factors, PV panel types, or aging. This adaptation is achieved through real-time monitoring of actual PV voltage and current values [18]. This algorithm operates by perturbing power and voltage at the PV module's output to precisely identify the optimal operational point, achieved by increasing or decreasing the duty cycle of the DC-DC converter [19], [20]. Each MPPT technique has distinct strengths and considerations, and the choice of method depends on the specific requirements of the solar power battery charging system.

Various efficient approaches have been explored for battery charging management. A study in [9] proposed a multi-stage charging system with impressive charge controller efficiency, aligning with commercial solar PV MPPT charge controller specifications. Another research in [21] introduced a Single-Ended Primary-Inductor Converter (SEPIC) as an MPPT charge controller for standalone PV systems. The SEPIC converter efficiently extracts maximum power from the PV array and adapts to irradiation changes [22]. These advancements enhance solar energy systems' sustainability and effectiveness.

In summary, the above literature provides a comprehensive explanation of the P&O MPPT method and its efficacy in maximizing battery charging. This paper aims to further investigate and enhance the storage modeling of the solar PV MPPT charge controller using MATLAB/Simulink. It explores the different performance characteristics of various battery types in terms of charging time and the amount of energy they can store. The organization of this paper is as follows: Section 2 presents the solar power charging system description, which includes the PV modeling and DC-DC converter. In Section 3, the proposed design of the Perturbation and Observation (P&O) algorithm and the battery controller subsystem are presented. In Section 4, the simulation results and discussions are provided, including the performance analysis of the proposed P&O technique and a comparison between Lead-acid and Lithium-ion batteries. Finally, Section 5 concludes the study, summarizing the observations and insights gained from the results obtained.

2. SOLAR POWER CHARGING SYSTEM DESCRIPTION

2.1 PV Charging System Description and Modelling

Figure 1 illustrates the PV charging system equipped with a controller for Maximum Power Point Tracking (MPPT). The design of the photovoltaic system is segregated into two main components: the modeling of the photovoltaic array and the modeling of the MPPT buck DC-DC converter. The solar irradiation contributes to the PV power that charges the battery. Any surplus energy beyond the load's needs is directed towards the battery charging process, ensuring efficient energy utilization. In situations where user power demand exceeds supply, the battery storage system fulfills the additional energy requirements.

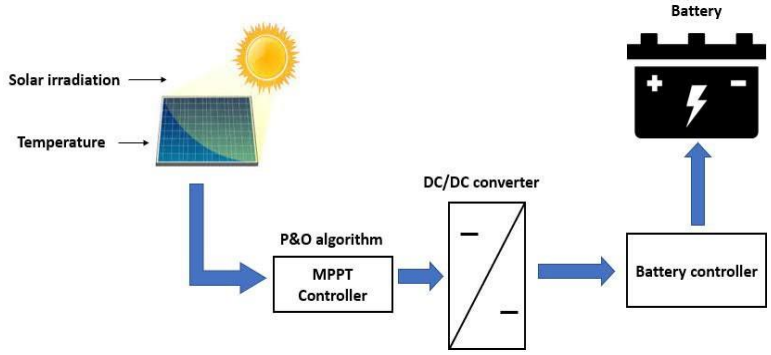

Figure 1. PV Charging System with Maximum Power Point Tracking (MPPT) controller

2.2 PV Panel Model

Figure 2 depicts the circuitry of the solar cell model, encompassing components such as photocurrent, diode, parallel resistor, and series resistor. The circuit comprises a current source, I_{ph}, representing the cell's photo-current, alongside shunt resistance (R_{pm}), series resistance (R_{sm}), and a diode. Typically, R_{pm} is of significant magnitude, while R_{sm} is considerably smaller, allowing them to be disregarded for analytical simplification. In practical applications, photovoltaic cells are aggregated into larger entities known as PV modules, and these modules can be interconnected in either series or parallel configurations to construct PV arrays, which form the backbone of electricity generation in photovoltaic systems [18].

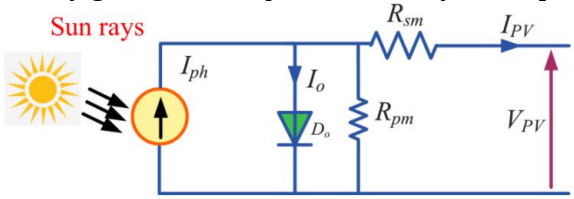

Figure 2. Single diode PV cell equivalent circuit.

From the equivalent circuit, consequently, a PV array I-V characteristic equation can be represented as follow,

$$I_{PV} = I_{ph} - I_O\left[exp\left(\frac{V_{PV} + R_S I_{PV}}{V_t a}\right) - 1\right] - \frac{V_{PV} + R_{sm} I_{PV}}{R_{pm}} \quad (1)$$

In this context, some key terms are defined: V_{PV} and I_{PV} stand for the output voltage and current of the PV cell respectively; I_{ph} represents the photocurrent, while I_O signifies the saturation current. Additionally, $V_t = k\,T/q$ is used to represent the thermal voltage of the PV cell, where q denotes the electron charge ($q = 1602 \times 10^{-19}$ C), k is the Boltzmann constant ($k = 1380 \times 10^{-23}$ J/K), and T indicates the temperature of the p-n junction. The parameter a corresponds to

the ideality factor of the diode. Meanwhile, the parallel resistance of the PV cell is noted as R_{pm}, and the series resistance is denoted by R_{sm}

The magnitude of the photocurrent is predominantly influenced by the solar PV radiation's intensity and the temperature of the PV cells. This relationship can be mathematically expressed as:

$$I_{ph} = \left(I_{sc} + k_i(T_c - T_{stc})\right)\left(\frac{G}{G_{stc}}\right) \tag{2}$$

In this scenario, consider the situation where the photocurrent generated under Standard Test Conditions (STC) is referred to as I_{ph}. The temperature and irradiance at STC are represented as T_{stc} (25°C) and G_{stc} (1000 W/m^2) respectively. Additionally, k_i represents the short circuit current coefficient, a parameter often supplied by the manufacturer. Alternatively, the diode's saturation current can be acquired using the subsequent equation:

$$I_o = \frac{I_{ph} + k_i(T_c - T_{stc})}{\exp\left(\frac{V_{OC} + k_v(T_c - T_{stc})}{aV_t}\right) - 1} \tag{3}$$

where the open circuit voltage at STC is V_{OC} and the open circuit coefficient is k_v. These parameters are accessible within the datasheet. For the MATLAB/Simulink model in this study, the 1Soltech 1STH-215-P photovoltaic module is employed. This module is constructed from multicrystal silicon solar cells configured in 2 parallel strings, with 2 series-connected modules per string. Its specified maximum power output stands at 213.15W.

2.3 DC-DC Converter

When performing calculations for the converter, numerous parameters come into consideration, including switching frequency, duty cycle, values of inductance and capacitance, output voltage ripple, inductor current, and output voltage. Given the lower battery voltage compared to the PV array, a buck topology is well-suited for solar PV charge controller application. The literature encompasses multiple past studies on various buck converters [18], [23], [25]. This choice stems from the buck converter's role as a regulator, reducing the input voltage from the PV array while ensuring the battery receives adequate power for charging. The fundamental DC-DC buck converter topology is presented in Figure 3, comprising a controlled switch S_w, an uncontrolled diode (D), an inductor L, a capacitance C, and a load resistance R.

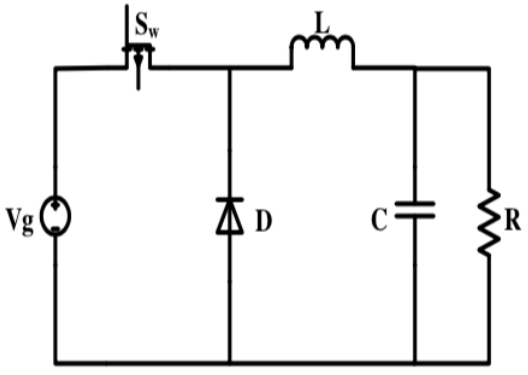

Figure 3. DC-DC buck converter topology.

The resulting current can be established by comparing the power (P) derived from the PV solar input with the battery's output voltage (V_o). A current ripple of about 10% of the output current can be hypothesized. The switching frequency is set at 5 kHz, and the voltage ripple is defined at 1% [23].

$$\text{Output current (A)} = \frac{P}{V_o} \tag{4}$$

$$\text{Inductance (L)} = \frac{V_o(V_g - V_o)}{f_{sw} \times I_{ripple} \times V_g} \tag{5}$$

$$\text{Capacitance (C)} = \frac{I_{ripple}}{8 \times f_{sw} \times V_{ripple}} \tag{6}$$

$$D = \frac{V_o}{V_g} \tag{7}$$

Where V_o is output voltage, V_g is input voltage of solar cell, D is duty cycle, P is solar cell power and f_{sw} is switching frequency.

3. PERTURB AND OBSERVE (P&O) MPPT ALGORITHM FOR PV CHARGING SYSTEM

3.1 Perturb and Observe Algorithm

In this section, the proposed Perturb and Observe (P&O) algorithm for this research's scope is discussed. Broadly speaking, the P&O algorithm plays a vital role in ensuring that the generated energy from the PV system consistently operates at its optimum, irrespective of solar irradiance and temperature conditions, thus ensuring efficient battery charging. This algorithm's function relies on the power and voltage at the PV module's output. For achieving the maximum power point (MPP), as depicted in Figure 4, a sequence of steps is followed. Initially, at point 1, when the arrow descends (i), both power and voltage decrease. To attain the MPP, an increase in power is necessary. This can be achieved by elevating the voltage while reducing the duty cycle. Conversely, as indicated by the upward movement along the curve at point 1 (ii), to achieve the MPP, the duty cycle should decrease while the voltage increases. This strategic manipulation ensures reaching the MPP effectively. Subsequently, considering point 2, there's a decrease in power alongside an increase in voltage (iv). Additionally, there's a visible power increase with a concurrent voltage decrease (iii). In this scenario, the duty cycle should be elevated, paired with a voltage reduction. An encapsulation of the P&O operation particulars can be found in Table 1.

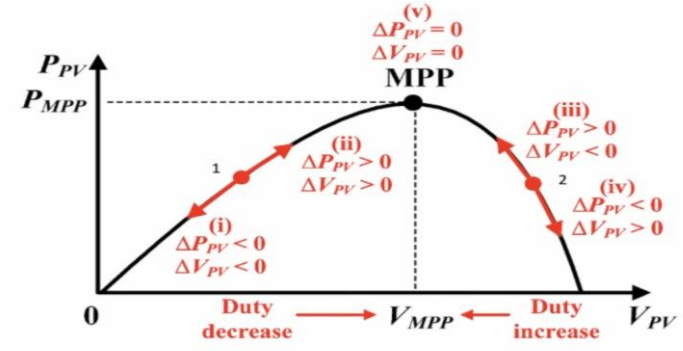

Figure 4. Power versus Voltage for MPP curve

Table 1 The operation of P&O algorithm.

ΔPpv	ΔVpv	**Perturbation**
> 0	> 0	At point 1 (ii), Increase V (by decrease duty cycle)
> 0	< 0	At point 2 (iii), Decrease V (by increase duty cycle)
< 0	> 0	At point 2 (iv), Decrease V (by increase duty cycle)
< 0	< 0	At point 1 (i), Increase V (by decrease duty cycle)

In this proposed approach, the system's power output is examined by altering the supply originating from the output PV panel. As this method only necessitates the sensing of voltage, its implementation is straightforward. The power output of the system is assessed through variations in the supplied voltage. If augmenting the voltage (V) concurrently increases the power (P), the duty cycle (D) value is further augmented; otherwise, the duty cycle (D) value is reduced. Similarly, while voltage reduction leads to power increase, the duty cycle is diminished. This sequence of actions persists until the maximum power point is achieved. The complete procedure of the P&O algorithm is illustrated in Figure 5.

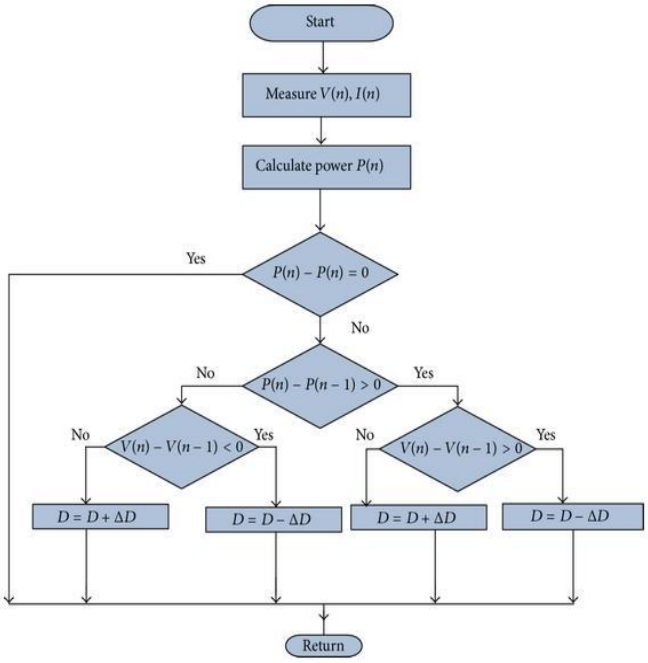

Figure 5. The flowchart of the P&O algorithm method.

3.2 Battery Charge Controller

In this presented work, after designing the P&O algorithm effectively to ensure that the generated output power from the PV module consistently remains at its optimal level, the system is then connected to a load, which in this case, is the battery charging load. Consequently, equal attention needs to be given to the methodology of controlling battery charging. Illustrated by the flowchart in Figure 6, the process of battery control within the solar power charging system is explained. The battery control assesses the battery's State of Charge (SOC) percentage. The battery's SOC is maintained at 80% for full charge. If the battery's charging reaches 80% SOC, it will discharge until it reaches 60% SOC; otherwise, it will remain in the charging state. Subsequently, if the SOC drops below the minimum value of 60%, the battery will commence charging until reaching 80% SOC. Figure 6 portrays the flowchart for charging and discharging battery controller. During charging, the pulse becomes one, triggering the circuit switch for battery control. Similarly, during

discharging, the pulse becomes zero. During this continuous process, the battery is precisely controlled and charged to maintain it at its optimal level.

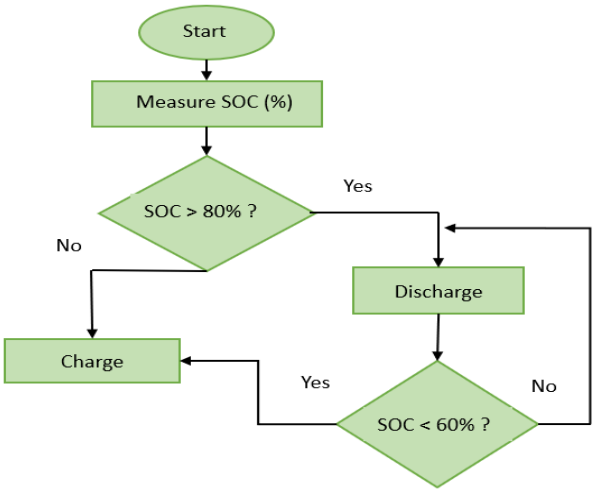

Figure 6. The flowchart of the battery control in MATLAB Simulink

4. RESULT AND DISCUSSION

4.1 Proposed Circuit Design in MATLAB Simulink

The circuit design for the buck converter and battery control has been comprehensively developed using the MATLAB/Simulink software, as depicted in Figure 7. This design encompasses key components including the PV array, P&O MPPT algorithm, DC-DC buck converter, and the battery system. In this configuration, four ideal switches have been incorporated to precisely regulate the charging process of the lead-acid battery. For PV control, the MPPT with P&O algorithm is utilized to ensure optimal energy harvesting from the PV panel. This algorithm constantly adapts to varying conditions, maximizing the output power from the solar array. On the other hand, the battery control system not only manages the battery during the charging process but also executes multi-stage charging. This multi-stage approach enhances the overall battery charging efficiency and longevity.

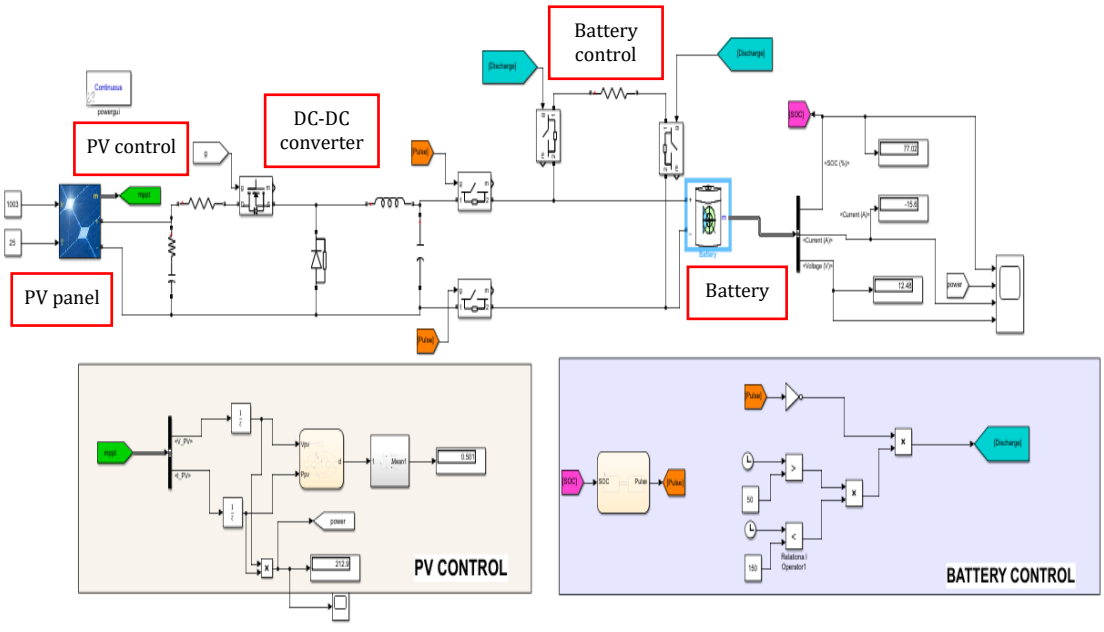

Figure 7. Circuit design in MATLAB Simulink

4.2 Data for battery charging in different irradiance

The crucial dataset used as input for the PV panel analysis was acquired through a diligent collaboration with the UiTM Green Energy Research Centre (GERC). This comprehensive dataset, selected by the specialized solar division of UiTM (GERC) [24], spans a significant time-based window, commencing from 11 am and extending through 2 pm. This timeline encapsulates the dynamic solar irradiance variations throughout this interval. It is important to note that solar irradiance (expressed in W/m^2) is an essential determinant of power generation efficiency. As the solar irradiance intensifies, a tangible increase in power output (measured in W) is concurrently observed. This characterized interrelation between solar irradiance and power output finds its expression in the graphical representation offered by Figure 8, a comprehensive bar chart. This illustrative chart clearly emphasizes the noticeable impact of varying irradiance levels on the power generation potential of the solar panel. It becomes evident that an increase in irradiance causes a proportionate surge in the power harnessed by the solar panel. The maximum power of 213.3 W is generated when the solar irradiance is 1003 W/m^2. This relationship, where heightened solar irradiance creates amplified power output, is at the core of solar energy harnessing. Thus, it views that an elevation in solar irradiance invariably translates into a correlated elevation in the solar panel's power output.

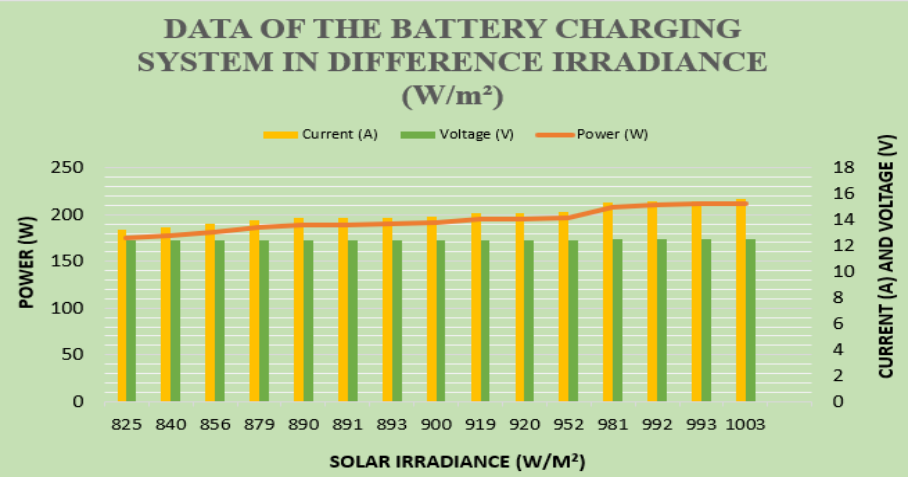

Figure 8. Bar chart for the data of the battery charging system

4.3 Multi-stage charging in Lead-acid battery

The multi-stage battery charging process is conducted under a solar irradiance condition of 1003 W/m^2, as depicted in Figure 9. This simulation commences with the battery's state of charge (SOC) at 78%, and it is set to reach 80% for a complete charge in lead-acid batteries. Stage 1 - Bulk Charging: This stage exhibits a constant current with an average of 14 A at 5 s, 10 s, and 15 s. Meanwhile, the voltage steadily increases from 0 s to 21 s, maintaining an SOC of 80%. Stage 2 - Absorption Charging: During this phase, the charging voltage remains constant. The outcomes indicate that when the battery reaches full charge, the current remains steady. This observation signifies that the battery is fully loaded, indicated by the voltage drop from 14V to 13V during the absorption stage. Stage 3 - Float Charging: As this stage unfolds, the battery is ready to discharge. The SOC graph experiences a decrease due to the discharging process. Furthermore, the current surges as it prepares to supply the load, reaching 10 A within the initial 51 s. Stage 4 - Equalization Charging: The equalization phase automatically triggers a new cycle of charging, ensuring the battery's health and balance. This step is a pivotal aspect of the multi-stage charging process, contributing to the optimal functionality and longevity of the battery.

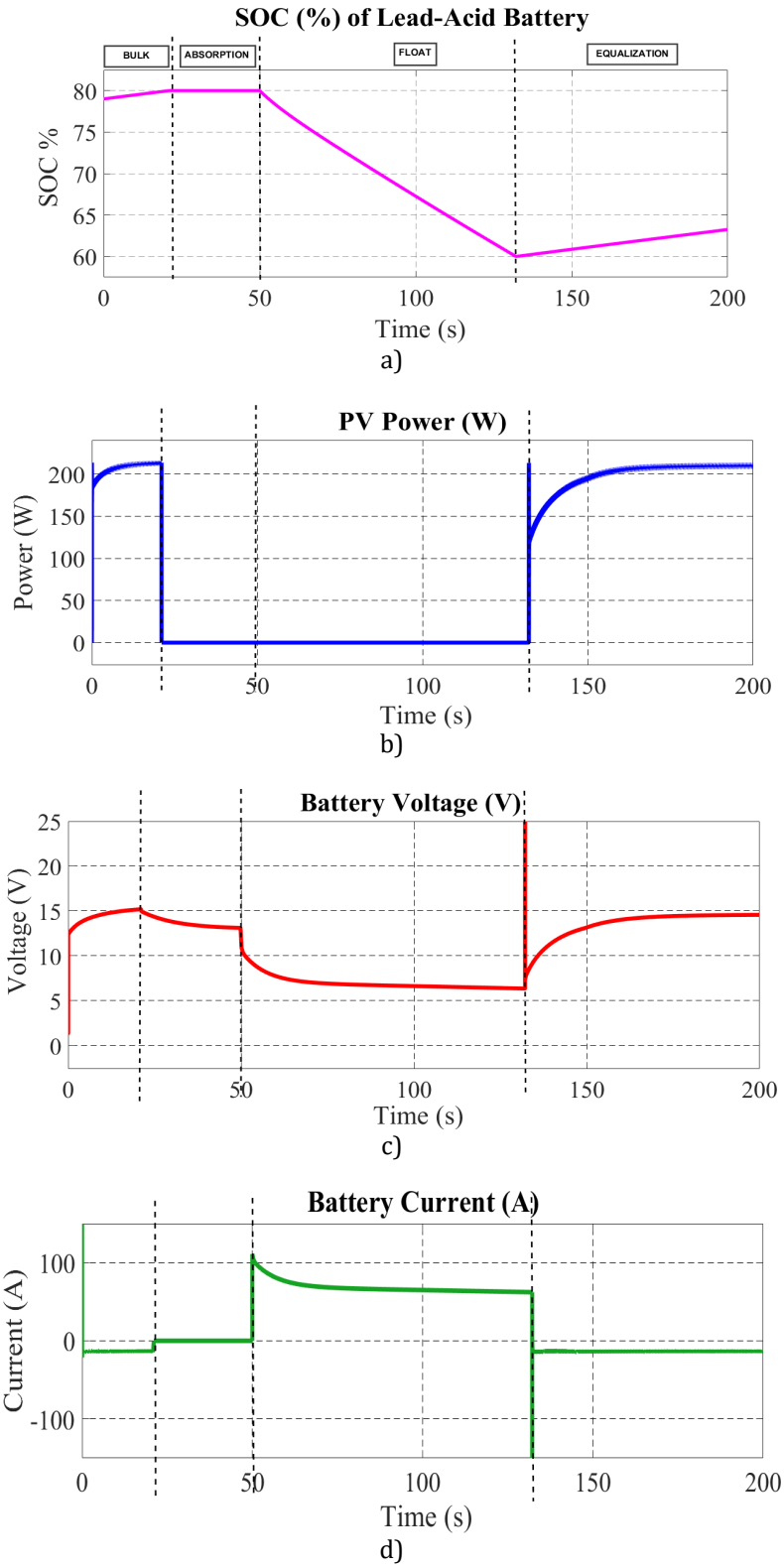

Figure 9. Output Battery charging and discharging: a) State of Charge SOC, b) power, c) voltage and d) current.

4.4 Comparison between Lead-acid and Lithium-ion battery

The outcomes presented in Figure 10 provide insights into the comparative performance of Lead-acid and Lithium-ion batteries. The analysis reveals that the Lead-acid battery requires 21 s to attain 80% of SOC, while the Lithium-ion variant accomplishes the same feat in a shorter span of 20 s. Additionally, during the discharging phase, the Lithium-ion battery demonstrates a time span of 50 s to 105 s, whereas the Lead-acid battery extends this timeframe to 50 s until 132 s. Upon observation, both battery types effectively store energy, each showcasing distinctive strengths and limitations. For instance, the Lithium-ion battery manages to discharge from a fully charged state to the minimum SOC of 60% in approximately 55 s, while the Lead-acid counterpart takes a longer duration of 82 s to reach the same minimum SOC level. This difference highlights the Lead-acid battery's larger capacity in contrast to the Lithium-ion alternative. Furthermore, in terms of the time required for full charging, the Lithium-ion battery surpasses the Lead-acid variant in speed. This is attributed to the considerably higher self-discharge rate of Lead-acid batteries, which is five times greater than that of their lithium counterparts. This attribute enhances the Lithium-ion battery's efficiency in terms of charging and discharging processes.

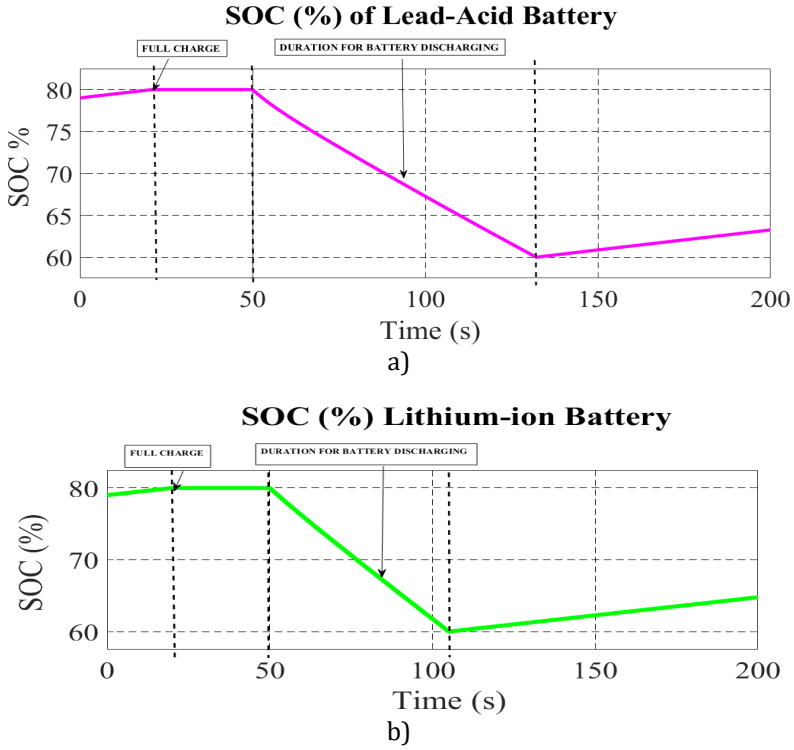

Figure 10. Output battery for charging and discharging: a) SOC of Lead-acid battery, b) SOC of Lithium-ion battery

Lithium-ion batteries offer several advantages. One notable benefit is their rapid charging time, which surpasses that of Lead-acid batteries. Moreover, they possess a higher energy density than other rechargeable batteries due to Lithium's propensity to shed electrons. This phenomenon is rooted in the fact that lithium carries only one electron in its outer shell, and it readily surrenders this electron due to its high reactivity as a metal [25]. The results depicted in Figure 10 affirm that Lithium-ion batteries exhibit a swifter response during the charging phase compared to Lead-acid batteries. This observation highlights the viability of Lithium-ion batteries as a robust solution for storing energy generated by solar panels. The outcomes also indicate that Lithium-ion batteries achieve full charge in a significantly shorter time than Lead-acid batteries. Given the unpredictable nature of sunlight, the rapid charge capability of Lithium-ion batteries becomes advantageous, enabling the system to capture more energy before weather conditions change.

5. CONCLUSIONS

This article presents the modeling of a solar power battery charging system with Maximum Power Point Tracking (MPPT) using the Perturb & Observe (P&O) algorithm. The effectiveness of the proposed MPPT design, along with the buck converter circuit and four-stage charge controller, is evaluated through MATLAB/Simulink simulation. The simulation results in Section 4 demonstrate that the maximum power of 213.3 W is generated when the solar irradiance is 1003 W/m^2. The battery's response in the storage system with multistage charging is clearly observed, distinguishing the bulk, absorption, float, and equalization stages. Battery control manages the battery's charging state, specifically by regulating the State of Charge (SOC) to a maximum of 80%. Afterward, the battery discharges to the lower SOC of 60%. This control is essential to prevent overcharging of the battery. Furthermore, the performance of different types of batteries is examined. The simulation uses both Lead-acid and Lithium-ion batteries, each having its advantages and disadvantages, particularly in terms of charging and discharging times.

ACKNOWLEDGEMENTS

The authors would like to extend their sincere appreciation and gratitude to the College of Engineering, Universiti Teknologi MARA (UiTM), and the Faculty of Electrical Engineering, Universiti Teknikal Malaysia Melaka (UTeM) and the Ministry of Higher Education (MOHE) Malaysia, for their unwavering support and encouragement throughout this research endeavor. Additionally, the authors would like to express their profound thanks to Bright Star University, el-Brega, Libya, for their invaluable contributions and collaboration, which have greatly enriched the scope and impact of this study. The successful completion of this research would not have been possible without the generous funding, guidance, and resources provided by these esteemed institutions, and for that, the authors remain deeply grateful.

REFERENCES

[1] R. S. Surender, P. Sravanthi, and K. Seong-Cheol, "Comprehensive analysis of current research trends in energy storage technologies," *Indonesian Journal of Electrical Engineering and Computer Science*, vol. 24, no. 3, pp. 1288–1296, 2021.

[2] M. Vaka, R. Walvekar, A. K. Rasheed, and M. Khalid, "A review on Malaysia's solar energy pathway towards carbon-neutral Malaysia beyond Covid'19 pandemic," *Journal of cleaner production*, vol. 273, pp. 122834, 2020.

[3] X. Li, T. Wu, H. J. Zhang, and D. Y. Yang, "National innovation systems and the achievement of sustainable development goals: Effect of knowledge-based dynamic capability," *Journal of Innovation & Knowledge*, vol. 8, no. 1, pp. 100310, 2023.

[4] R. Wang, S. C. Hsu, S. Zheng, J. H. Chen, and X. I. Li, "Renewable energy microgrids: Economic evaluation and decision making for government policies to contribute to affordable and clean energy," *Applied Energy*, vol. 274, pp. 115287, 2020.

[5] P. K. D. Pramanik *Et Al.*, "Power Consumption Analysis, Measurement, Management, And Issues: A State-Of-The-Art Review Of Smartphone Battery And Energy Usage," *IEEE Access*, vol. 7, no. December, pp. 182113–182172, 2019.

[6] G. A. M. Madrigal, K. G. Cuevas, V. Hora, K. M. Jimenez, J. N. Manato, M. J. Porlaje, and B. Fortaleza, "Fuzzy Logic-based Maximum Power Point Tracking Solar Battery Charge Controller with Backup Stand-by AC Generator," *Indonesian Journal of Electrical Engineering and Computer Science*, vol. 16, no. 1, pp. 136–146, 2019.

[7] J. He, J. Meng, and Y. Huang, "Challenges and recent progress in fast-charging lithium-ion battery materials," *Journal of Power Sources*, vol. 570, pp. 232965, 2023.

[8] D. Darbar, T. Malkowski, E. C. Self, I. Bhattacharya, M. V. V. Reddy, and J. Nanda, "An overview of cobalt-free, nickel-containing cathodes for Li-ion batteries," *Materials Today*

Energy, vol. 30, pp. 101173, 2022.
[9] S. F. Chevtchenko, E. J. Barbosa, M. C. Cavalcanti, G. M. Azevedo, and T. B. Ludermir, "Combining PPO and incremental conductance for MPPT under dynamic shading and temperature," *Applied Soft Computing*, vol. 131, pp. 109748, 2022.
[10] W. Hayder, A. Abid, M. B. Hamed, and L. Sbita, "Intelligenit MPPT algorithm for PV system based on fuzzy logic," *in 2020 17th International Multi-Conference on Systems, Signals & Devices (SSD)*, vol. 2020-July, pp. 239-243, 2020.
[11] A. G. Olabi, M. A. Abdelkareem, C. Semeraro, M. Al Radi, H. Rezk, O. Muhaisen, and E. T. Sayed, "Artificial neural networks applications in partially shaded PV systems," *Thermal Science and Engineering Progress*, vol. 37, no. 2023, pp. 101612, 2022.
[12] Y. Rais, A. Zakriti, and A. Khamlichi, "Maximum power point tracking in photovoltaics: Overview and application," *in 2018 Renewable Energies, Power Systems & Green Inclusive Economy (REPS-GIE)*, vol. 2018-April, pp. 1-6, 2018.
[13] A. M. Shaikh, M. F. Shaikh, S. A. Shaikh, M. Krichen, R. A. Rahimoon, and A. Qadir, "Comparative analysis of different MPPT techniques using boost converter for photovoltaic systems under dynamic shading conditions," *Sustainable Energy Technologies and Assessments*, vol. 57, pp. 103259, 2023.
[14] M. Alshareef, "An Improved MPPT Method Based on Fuzzy Logic Controller for a PV System," *Studies in Informatics and Control*, vol. 30, no. 1, pp. 89-98, 2021.
[15] S. Boualem, O. Kraa, M. Benmeddour, M. Kermadi, M. Maamir, and H. Cherif, "Power management strategy based on Elman neural network for grid-connected photovoltaic-wind-battery hybrid system," *Computers and Electrical Engineering*, vol. 99, pp. 107823, 2022.
[16] N. Kacimi, S. Grouni, A. Idir, and M. S. Boucherit, "New improved hybrid MPPT based on neural network-model predictive control-kalman filter for photovoltaic system," *Indonesian Journal of Electrical Engineering and Computer Science*, vol. 20, no. 3, pp. 1230-1241, 2020.
[17] C. G. Villegas-Mier, J. Rodriguez-Resendiz, J. M. Álvarez-Alvarado, H. Rodriguez-Resendiz, A. M. Herrera-Navarro, and O. Rodríguez-Abreo, "Artificial neural networks in MPPT algorithms for optimization of photovoltaic power systems: A review," *Micromachines*, vol. 12, no. 10, pp. 1260, 2021.
[18] C. S. Kumar, and G. Mallesham, "A new hybrid boost converter with P&O MPPT for high gain enhancement of solar PV system," *Materials Today: Proceedings*, vol. 57, pp. 2262-2269, 2022.
[19] B. S. V. Sai, S. A. Khadtare, and D. Chatterjee, "An improved weather adaptable P&O MPPT technique under varying irradiation condition," *ISA transactions*, 2023.
[20] R. Alik, and A. Jusoh, "An enhanced P&O checking algorithm MPPT for high tracking efficiency of partially shaded PV module," *Solar Energy*, vol. 163, pp. 570-580, 2018.
[21] M. A. Jusoh, M. F. N. Tajuddin, S. M. Ayob, And M. A. Roslan, "Maximum Power Point Tracking Charge Controller For Standalone Pv System," *Telkomnika (Telecommunication Comput. Electron. Control).*, vol. 16, no. 4, pp. 1413–1426, 2018.
[22] A. Chellakhi, S. El Beid, and Y. Abouelmahjoub, "An improved adaptable step-size P&O MPPT approach for standalone photovoltaic systems with battery station," *Simulation Modelling Practice and Theory*, vol. 121, pp. 102655, 2022.
[23] A. C. Subrata, T. Sutikno, S. Padmanaban, And H. S. Purnama, "Maximum power point tracking in PV arrays with high gain DC-DC boost converter," in *Int. Conf. Electr. Eng. Comput. Sci. Informatics*, no. September, pp. 358–362, 2019.
[24] S. Shaari, A. M. Omar, A. M., and M. Z. Hussin, "Simplified modeling techniques for predicting outputs of grid-connected photovoltaic power systems," *Journal of Renewable Energy and Smart Grid Technology*, vol. 9, no. 1, pp. 9-18, 2014.
[25] M. Veerachary, and P. Sen, "Dual-switch enhanced gain boost DC–DC converters," *IEEE Transactions on Industry Applications*, vol. 58, no. 4, pp. 4903-4913, 2022.